Microchim Acta (2015) 182:1933–1939
DOI 10.1007/s00604-015-1526-4

ORIGINAL PAPER

A near-infrared fluorescent bioassay for thrombin using aptamer-modified $CuInS_2$ quantum dots

Zihan Lin[1] · Dong Pan[2] · Tianyu Hu[1] · Ziping Liu[1] · Xingguang Su[1]

Received: 27 January 2015 / Accepted: 11 May 2015 / Published online: 26 May 2015

Abstract We describe a near-infrared (NIR) fluorescent thrombin assay using a thrombin-binding aptamer (TBA) and Zn(II)-activated $CuInS_2$ quantum dots (Q-dots). The fluorescence of Zn(II)-activated Q-dots is quenched by the TBA via photoinduced electron transfer, but if thrombin is added, it will bind to TBA to form G-quadruplexes and the Q-dots are released. As a result, the fluorescence intensity of the system is restored. This effect was exploited to design an assay for thrombin whose calibration plot, under optimum conditions, is linear in the 0.034 to 102 nmol L^{-1} concentration range, with a 12 pmol L^{-1} detection limit. The method is fairly simple, fast, and due to its picomolar detection limits holds great potential in the diagnosis of diseases associated with coagulation abnormalities and certain kinds of cancer.

Keywords $CuInS_2$ quantum dots · Near-infrared · Thrombin · Aptamer · Fluorescence

Zihan Lin and Dong Pan contributed equally to this work.

Electronic supplementary material The online version of this article (doi:10.1007/s00604-015-1526-4) contains supplementary material, which is available to authorized users.

✉ Xingguang Su
suxg@jlu.edu.cn

[1] Department of Analytical Chemistry, College of Chemistry, Jilin University, Changchun 130012, People's Republic of China

[2] State Key Laboratory of Supramolecular Structure and Materials, Jilin University, Changchun 130012, People's Republic of China

Introduction

Thrombin is a serine protease protein, which converts soluble fibrinogen into insoluble strands of fibrin, as well as catalyzing many other coagulation related reactions [1]. It is also related to a number of pathological processes, such as cardiovascular diseases, angiogenesis, inflammation, metastasis, and has been considered as a biomarker for tumor diagnosis [2]. The concentration of thrombin in blood varies considerably and can be virtually absent in healthy subjects. However, in the coagulation process, the concentration of thrombin in blood ranges from nM to low mM levels [3]. As the higher concentration of thrombin in blood is known to be relevant with some diseases [4], it is significant to be able to detect this enzyme accurately at trace levels. Therefore, even at picomolar range in blood thrombin is associated with diseases, thus requiring highly sensitive analytical protocols. So far, numerous approaches to detect thrombin have been developed, for instance, colorimetry [5], electrochemistry [6], and surface enhanced Raman spectroscopy (SERS) [7]. However, these methods cannot fulfill the demand for large-scale analysis, due to their limitations of being highly instrument dependent, having complicated sensing mechanisms, relatively high detection limits, narrow detection range, low sensitivity and expensive labeling substances. Thus, highly sensitive detection of thrombin is of immense importance for early diagnosis and monitoring.

Fluorescence detection has been extensively used as an analytical technique owing to its operational simplicity, high sensitivity and real-time detection. A series of fluorescence sensors have been designed for protein detection [8]. DNA or RNA oligonucleotide aptamers have a high affinity and specificity towards a variety of targets [9], however, most of these approaches involve tedious DNA labeling or modification techniques that are based on condensation reaction

between the carboxyl group and the amino group, or streptavidin–biotin specific reaction, etc. [10, 11]. These processes are usually technically demanding, time consuming, and expensive, and may also affect the affinity of the aptamer. Therefore, the development of aptamer based methods for thrombin detection is promising. Thrombin binding aptamer (TBA), owing to lots of advantages as the ease of labeling, excellent stability and high affinity and selectivity towards thrombin [12], has been widely used as a recognition element to construct thrombin biosensors combined with different analysis methods [13, 14]. The single-stranded DNA oligonucleotide, TBA, with 15 nucleotides was selected from a randomized oligonucleotide library as a high affinity ligand for thrombin [15]. A guanine-quartet based quadruplex structure, named "G-quartet structure", was formed when this aptamer binds to thrombin [16].

Near infrared quantum dots (NIR Q-dots) are promising fluorescent probes for several biomedical applications. However so far applications of NIR Q-dots to the clinical field have been hampered by the high toxicity of the NIR Q-dots such as Ag_2S [17], InAs/InP/ZnSe [18] and CuInSe/ZnS [19]. Most of NIR Q-dots are synthesized via an organometallic precursor route in an organic solvent that is hazardous to the environment and to the health of the people [20]. Thus the development of less toxic and more environmentally friendly ternary NIR Q-dots materials attracted considerable attention. Recently, a type of NIR I–III–VI $CuInS_2$ Q-dots material has been reported. As a new low toxic material, several approaches have been employed to prepare $CuInS_2$ Q-dots [21] that do not contain any Class A element (Cd, Pb, and Hg) or Class B element (Se and As). Based on our previous report [22], we synthesized water-dispersible $CuInS_2$ Q-dots capped with 3-mercaptopropionic acid (MPA). The activation of Q-dots is typically attributed to some forms of surface passivation [23]. Upon addition of Zn(II), surface defect states were passivated, and the $CuInS_2$ Q-dots were thus activated.

In this paper, we report a simple NIR fluorescence assay using aptamer TBA and Zn(II)-activated $CuInS_2$ Q-dots for the highly selective and sensitive detection of thrombin, as shown in Scheme 1. The fluorescence of Zn(II)-activated $CuInS_2$ Q-dots is effectively quenched by TBA via the photo-induced electron transfer (PET) process. The TBA is known to form a stable G-quadruplex structure binding to thrombin, which adopts a specific three-dimensional "chair structure" [24]. Due to the strong specific binding interactions between TBA and thrombin, the addition of thrombin to the Zn(II)-activated $CuInS_2$ Q-dots system would disrupt the interaction between Zn(II)-activated $CuInS_2$ Q-dots and TBA, leading to the recovery of the fluorescence. This method for thrombin assaying has advantages of easy operation due to the elimination of complicated covalent modifications. The absence of modification ensures the free conformational change of the TBA when interacting with thrombin, thus leading to high binding affinity and sensitive detection. Therefore, this method was highly sensitive and selective in thrombin assaying.

Experimental

Materials

All chemicals used were of analytical reagent grade without further purification. Copper(II) chloride dehydrate ($CuCl_2$ $2H_2O$), sulfourea (CS $(NH_2)_2$) and sodium hydroxide (NaOH) were purchased from Beijing Chemical Works (http://ccesl.en.wdtrade.com). Mercaptopropionic acid (MPA) and indium(III) chloride tetrahydrate ($InCl_3$ •$4H_2O$), 2-Amino-2-(hydroxymethyl)-1,3-propanediol (Tris),

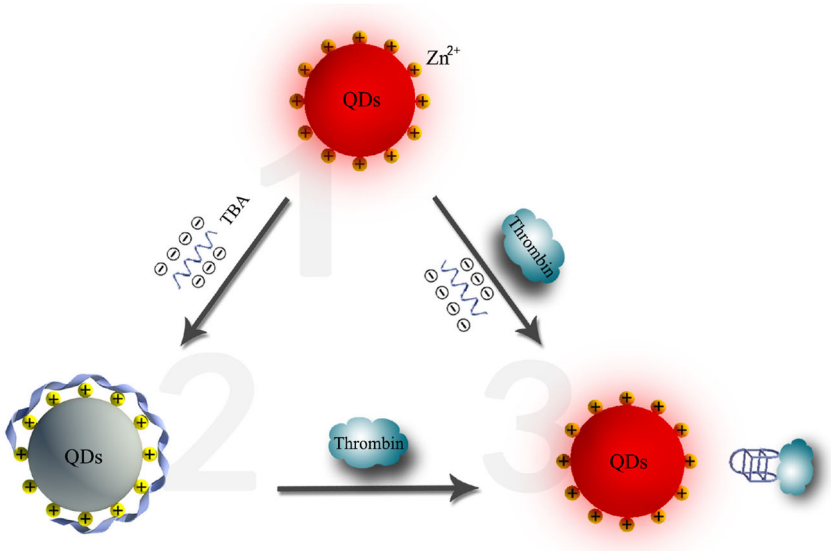

Scheme 1 Illustration of the mechanism for thrombin detection with Zn(II)-activated $CuInS_2$ Q-dots probe.

thrombin, bovine serum albumin (BSA), trypsin (Try), pepsin (Pep), immunoglobin G (IgG), hemoglobin (Hb) and lysozyme were purchased from Sigma-Aldrich Corporation (http://www.sigmaaldrich.com). 15-mer thrombin binding aptamer (TBA) with the sequence of 5′-GGTTGGTGTGGT TGG-3′ was synthesized by Sangon Biotechnology Co. (http://www.sangon.com), Ltd. The water used in the study had a resistivity higher than 18 MΩ cm. The 0.1 mol L^{-1} Tris–HCl buffered solution (pH 7.4) was used as the medium for detection process.

Instruments

Fluorescence measurements were performed on a Shimadzu RF-5301 PC spectrofluorophotometer (Shimadzu Co., Kyoto, Japan, http://www.shimadzu.com), and a 1 cm path-length quartz cuvette was used in experiments. All pH measurements were taken with a PHS-3C pH meter (Tuopu Co., Hangzhou, China, http://www.lei-ci.com).

Preparation of $CuInS_2$ Q-dots

NIR $CuInS_2$ Q-dots were prepared in aqueous solution via a hydrothermal synthesis method based on our previous report [22]. In a typical experiment, $CuCl_2$ $2H_2O$ (0.15 mmol) and $InCl_3$ $4H_2O$ (0.15 mmol) were dissolved in distilled water (10.5 mL), then MPA (1.8 mmol) was injected into the solution. The pH value of the mixture solution was adjusted to 11.3 by adding 2 mol L^{-1} NaOH solution with stirring. After stirring for 10 min, $CS(NH_2)_2$ (0.30 mmol) was dissolved in the solution. The Cu–to–In–to–S and Cu–to–MPA precursor ratios were 1 : 1 : 2 and 1 : 12, respectively. All the above mentioned experimental procedures were performed at room temperature, and then the solution was transferred into a Teflon-lined stainless steel autoclave with a volume of 15 mL. The autoclave was maintained at 150 °C for 21 h and then cooled down to room temperature. The fluorescence intensity of the MPA-capped $CuInS_2$ Q-dots solution stored in the dark for 1 month remains unchanged. The final concentration of the $CuInS_2$ Q-dots solution was calculated to be 0.79 μmol L^{-1} by using Lambert-Beer's law according to the previous reports [25, 26]. The fluorescence quantum yield of the $CuInS_2$ Q-dots synthesized was 3.3 %, which was higher than that synthesized in organic solvent (QY=3 %) [27].

The detection process

The $CuInS_2$ Q-dots were activated as following: $CuInS_2$ Q-dots (500 μL, 0.79 μmol L^{-1}) and Zn(II) (40 μL, 1 mmol L^{-1}) were successively added into 2.0 mL calibrated test tubes, then diluted to the mark with 10 mmol L^{-1} Tris–HCl buffer solution (pH 7.4) and mixed thoroughly for 10 min at room temperature, followed by recording the fluorescence spectrum of solution. At an excitation wavelength of 590 nm, the fluorescence spectra of the Zn(II)-activated $CuInS_2$ Q-dots were recorded in the 610–800 nm emission wavelength range.

After $CuInS_2$ Q-dots activation was finished, a series of different concentrations of TBA (from 0 to 810 nmol L^{-1}) were sequentially added to a 2 mL calibrated test tube, shaken thoroughly and equilibrated for 15 min, diluted to the mark with 10 mmol L^{-1} Tris–HCl buffer solution (pH 7.4). The fluorescence spectra were recorded from 610 to 800 nm, and the fluorescence intensity of the maximum emission peak was used for quantitative analysis of the TBA. All data were collected from at least three independent measurements.

The thrombin assay was carried out as follows: Zn(II)-activated $CuInS_2$ Q-dots-TBA and different concentrations of thrombin were sequentially added to a 2 mL calibrated test tube, shaken thoroughly and equilibrated at 37 °C for 40 min, diluted to the mark with 10 mmol L^{-1} Tris–HCl buffer solution (pH 7.4). The fluorescence spectra were recorded from 610 to 800 nm, and the fluorescence intensity of the maximum emission peak was used for quantitative analysis. All data were collected from at least three independent measurements.

Detection of thrombin in human blood serum

For serum samples detection, drug-free human blood samples were collected from healthy volunteer at the Hospital of Changchun China–Japan Union Hospital. All experiments were performed in compliance with the relevant laws and institutional guidelines, and the writing of informed consent for all samples was obtained from human subjects. All the blood samples were obtained through venipuncture and centrifuged at 9400 g for 10 min after standing for 2 h at room temperature. The serum samples were diluted ten times with Tris–HCl solution before detection. Dilution of human serum is a commonly pretreatment procedure for protease detection in samples of high complexity [28, 29].

Results and discussion

Feasibility of the thrombin assay system

The fluorescence emission spectra of $CuInS_2$ Q-dots, Zn(II)-activated $CuInS_2$ Q-dots ($CuInS_2$ Q-dots-Zn(II)), $CuInS_2$ Q-dots-Zn(II)-TBA and $CuInS_2$ Q-dots-Zn(II)-TBA-thrombin were shown in Fig. 1. It can be seen that the width of $CuInS_2$ Q-dots fluorescence spectrum was narrow, indicating the $CuInS_2$ Q-dots were nearly monodisperse and homogeneous. The fluorescence emission of the $CuInS_2$ Q-dots is enhanced significantly with the addition of Zn(II), which was due to the effective passivation of surface defects on the $CuInS_2$ Q-dots. The fluorescence of the $CuInS_2$ Q-dots-Zn(II) was quenched when it interacts with the negatively charged

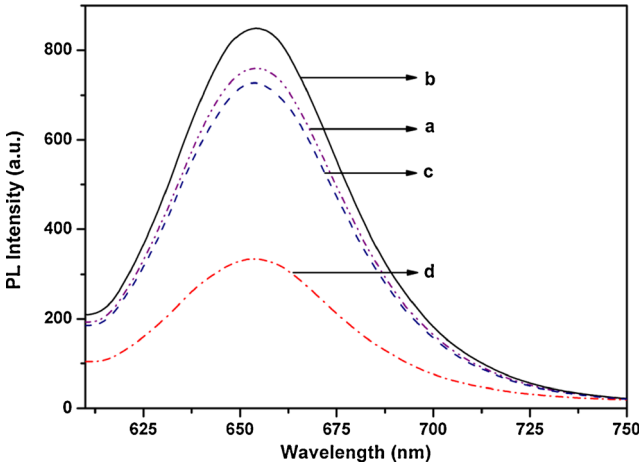

Fig. 1 The PL emission spectra of the $CuInS_2$ Q-dots (**a**), $CuInS_2$ Q-dots-Zn(II) (**b**), $CuInS_2$ Q-dots-Zn(II)-TBA (**c**) and $CuInS_2$ Q-dots-Zn(II)-TBA-thrombin (**d**). Excitation wavelengths: 590 nm, emission wavelength: 655 nm. All the experiments were performed in the 10 mmol L^{-1} Tris–HCl buffer solution (pH 7.4)

TBA (720 nmol L^{-1}) through photoinduced electron transfer (PET) process. When thrombin (102 nmol L^{-1}) was added, the TBA was induced to form G-quadruplexes which bound with thrombin owing to the specific binding interactions [30], and the $CuInS_2$ Q-dots-Zn(II) was released with an increase of fluorescence intensity. Based on the fluorescent signal changes of $CuInS_2$ Q-dots-Zn(II) when TBA specifically interacted with thrombin, detection of thrombin was achieved. Fig. S1 (Electronic Supplementary Material, ESM) shows the transmission electron microscopy (TEM) micrograph of $CuInS_2$ Q-dots. It can be seen that the size distribution of $CuInS_2$ Q-dots was reasonably uniform. The particle size of $CuInS_2$ Q-dots was approximate 2 nm. Fig. S2 (ESM) shows the FT-IR spectra of $CuInS_2$ Q-dots. As shown in Fig. S2, the majority of MPA functional groups were clearly found through the C=O stretching peak (1730 cm^{-1}), and C–H stretching mode (2850, 2920, 2960 cm^{-1}). The characteristic peak of S–H did not appear within 2550–2680 cm^{-1}, which might be caused by the covalent bonds between thiols and metal. In addition, the reproducibility of $CuInS_2$ Q-dots was also been studied. As shown in Fig. S3 (ESM), the fluorescence intensity of $CuInS_2$ Q-dots was almost constant in different batches.

Interactions between TBA and Zn(II)-activated $CuInS_2$ Q-dots

The fluorescence intensity of the Zn(II)-activated $CuInS_2$ Q-dots solution was obviously quenched upon addition of TBA. The fluorescence quenching of the $CuInS_2$ Q-dots-Zn(II) system in the presence of negatively charged TBA might suffer an effective PET process. The G-rich bases of TBA would act as an electron acceptor and lead to nonradiative electron–hole recombination annihilation [31]. Although fluorescence quenching was also observed in the original $CuInS_2$ Q-dots solution without Zn(II) activation, the fluorescence intensity changes of Zn(II)-activated $CuInS_2$ Q-dots upon addition of TBA was evidently greater than that of the original $CuInS_2$ Q-dots, as depicted in Fig. 2. This further proved that the interactions between $CuInS_2$ Q-dots and TBA were dominated by the electrostatic forces between the cationic Zn(II)-activated $CuInS_2$ Q-dots surface and the negatively charged TBA backbone.

The fluorescence quenching induced by the TBA

In this paper, we investigated systematically the fluorescence quenching of $CuInS_2$ Q-dots-Zn(II) induced by TBA. The fluorescence spectra of $CuInS_2$ Q-dots-Zn(II) in the presence of different concentrations of TBA were illustrated in Fig. 3. As shown in Fig. 3, the fluorescence intensity of $CuInS_2$ Q-dots-Zn(II) gradually decreased with the increasing of TBA concentration in the range of 0 to 810 nmol L^{-1}. Figure 3 inset revealed a good linear correlation between F/F_0 (F_0 is the fluorescence intensity of $CuInS_2$ Q-dots-Zn(II) and F is the fluorescence intensity of $CuInS_2$ Q-dots-Zn(II) system with the addition of different concentrations of TBA) and TBA concentration in the range of 36 to 720 nmol L^{-1}. The regression equation is: $F/F_0=1.009–8.2336\ C_{TBA}$, nmol L^{-1}. The regression coefficient is 0.995, and the detection limit (LOD) for TBA was calculated to be 16 nmol L^{-1}. The detection limit is calculated by the equation $LOD=(3\sigma/s)$ [32], where σ is the standard deviation of blank signals (n=9) and s is the slope of the calibration curve.

Optimization of method

The following parameters were optimized: (a) incubation time; (b) pH; (c) temperature. Respective data and Figures are given in the Electronic Supporting Material. The

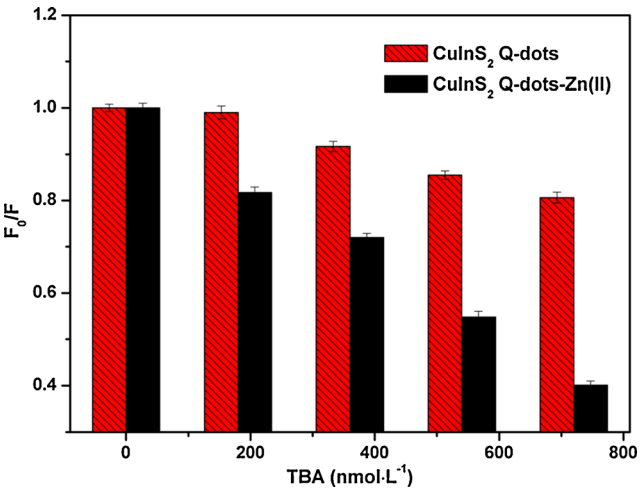

Fig. 2 Comparison of the quenching effects of TBA on the fluorescence of the original $CuInS_2$ Q-dots and the Zn(II)-activated $CuInS_2$ Q-dots. (F_0 and F are the fluorescence intensity before and after TBA was added, respectively.)

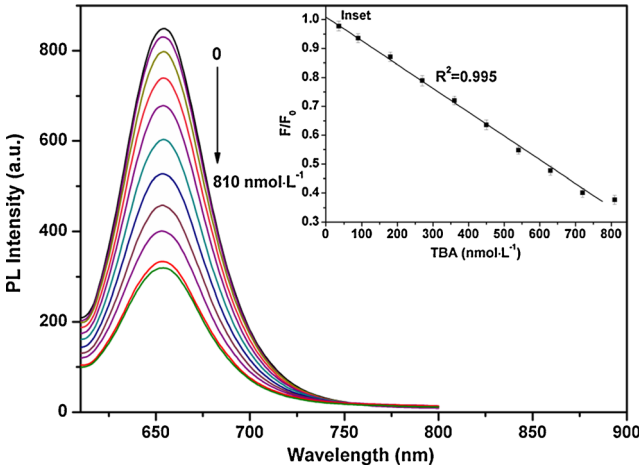

Fig. 3 The fluorescence spectra of $CuInS_2$ Q-dots-Zn(II) (0.2 μmol L^{-1}) system in the presence of different concentrations of TBA (0, 36, 90, 180, 270, 360, 450, 540, 630, 720, 810 nmol L^{-1}). Inset shows the linear relationship between F/F_0 and the concentration of TBA (from 36–720 nmol L^{-1}). F_0 is the fluorescence intensity of $CuInS_2$ Q-dots-Zn(II) and F is the fluorescence intensity of $CuInS_2$ Q-dots-Zn(II) after the addition of different concentrations of TBA. Reaction conditions: 10 mmol L^{-1} Tris–HCl buffer solution (pH 7.4) at 37 °C incubated for 15 min

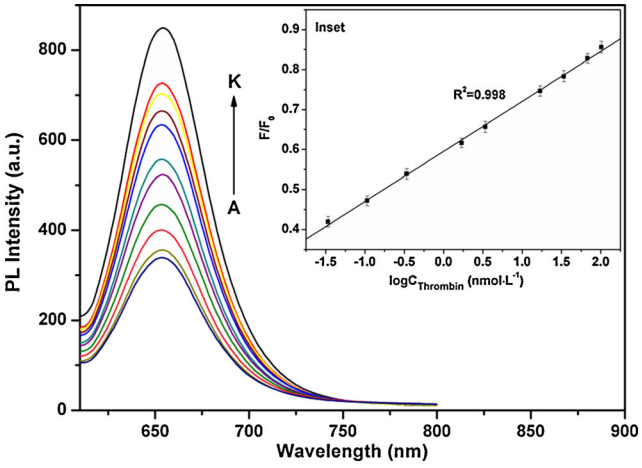

Fig. 4 The fluorescence spectra of 0.2 μmol L^{-1} $CuInS_2$ Q-dots-Zn(II) (**a**) and 0.2 μmol L^{-1} $CuInS_2$ Q-dots-Zn(II)-720 nmol L^{-1} TBA system upon the addition of different concentrations of thrombin. B–K represent the concentrations of thrombin of 0, 0.034, 0.17, 0.34, 1.7, 3.4, 17, 34, 68 and 102 nmol L^{-1}. Inset shows the relationship between F/F_0 and the concentration of thrombin. F_0 is the fluorescence intensity of $CuInS_2$ Q-dots-Zn(II) and F is the fluorescence intensity of $CuInS_2$ Q-dots-Zn(II)-TBA with the addition of different concentration of thrombin. Reaction conditions: 10 mmol L^{-1} Tris–HCl buffer solution (pH 7.4) at 37 °C incubated for 40 min

following experimental conditions were found to give best results: (a) a reaction time of 40 min (Fig. S4, ESM); (b) a sample pH value of 7.4 (Fig. S5, ESM); (c) a temperature of 37 °C (Fig. S6, ESM).

The thrombin detection

It can be seen from Fig. S7 (ESM) that the fluorescence intensity of $CuInS_2$ Q-dots-Zn(II) was not influenced by the addition of thrombin in the concentration range from 1.7 to 102 nmol L^{-1}, which indicated that the interaction between thrombin and $CuInS_2$ Q-dots was negligible. Figure 4 showed the fluorescence spectra of $CuInS_2$ Q-dots-Zn(II)-TBA system in the present of different concentrations of thrombin. When thrombin was added, the TBA was induced to form G-quadruplexes which bound with thrombin due to the specific binding interactions, leading to the recovery of the fluorescence intensity of $CuInS_2$ Q-dots-Zn(II). Figure 4 inset revealed a linear relationship between the relative fluorescence intensity ratio F/F_0 and thrombin concentrations in the range of 0.034 to 102 nmol L^{-1}. The regression equation is: $F/F_0=0.5952+0.1252 \log C_{Thrombin}$, nmol L^{-1}. The regression coefficient is 0.998, and the detection limit (LOD) for thrombin was calculated to be 0.012 nmol L^{-1}. A comparison between the method and other reported methods for thrombin determination with regards to detection limit and linear range is summed up in Table S1 (ESM). From Table S1, it can be seen that the sensitivity of this method was better than that of most of the well-known methods.

Interference study

As shown in Fig. 5, the fluorescence intensity of $CuInS_2$ Q-dots-Zn(II)-TBA (blank) was studied in the presence of 102 nmol L^{-1} thrombin, and of 1 mmol L^{-1} of each BSA, IgG,, hemoglobin, lysozyme, trypsin,and pepsin. The concentration of $CuInS_2$ Q-dots-Zn(II) is 0.2 μmol L^{-1} and the concentration of TBA is 720 nmol L^{-1} in the $CuInS_2$ Q-dots-Zn(II)-TBA system. Under the reaction conditions (10 mmol L^{-1} Tris–HCl buffer solution (pH 7.4) at 37 °C incubation for

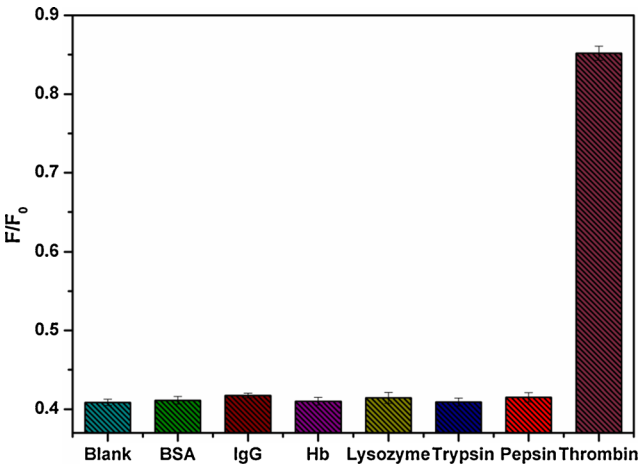

Fig. 5 The fluorescence intensity of $CuInS_2$ Q-dots-Zn(II)-TBA (Blank) in the presence of 102 nmol L^{-1} thrombin, 1000 nmol L^{-1} BSA, IgG, Hb, lysozyme, trypsin, and pepsin. The concentration of $CuInS_2$ Q-dots-Zn(II) is 0.2 μmol L^{-1} and the concentration of TBA is 720 nmol L^{-1} in the $CuInS_2$ Q-dots-Zn(II)-TBA system. Reaction conditions: 10 mmol L^{-1} Tris–HCl buffer solution (pH 7.4) at 37 °C incubated for 40 min

Table 1 Determination of thrombin in human serum samples

Serum samples	Added thrombin (nmol L^{-1})	Found (nmol L^{-1})	Recovery (%)	RSD (%, n=3)
1	1.71	1.76	103	2.9
2	3.42	3.59	105	3.2

40 min), the following data for F/F_0 were obtained: Blank: $CuInS_2$ Q-dots-Zn(II) 0.2 μmol L^{-1}, TBA 720 nmol L^{-1}; BSA: 1 mmol L^{-1}; IgG: 1 mmol L^{-1}; hemoglobin: 1 mmol L^{-1}; lysozyme: 1 mmol L^{-1}; trypsin: 1 mmol L^{-1}; pepsin: 1 mmol L^{-1}; thrombin: 102 nmol L^{-1}.

We further tested this assay system with several potentially interfering ions. As shown in Table S2 (ESM), the tolerable concentrations of the $CuInS_2$ Q-dots-Zn(II)-TBA system towards interfering ions were all beyond the concentration ranges in healthy subjects. A relative error of ±5.0 % was considered to be tolerable. These results revealed that the approach developed here has a highly selective response toward thrombin, free from the interference of common potentially interfering ions or proteins.

Detection of thrombin in human serum samples

In order to demonstrate the feasibility of the method, it was applied to the determination of thrombin in human serum samples. Serum is what remains from whole blood after coagulation, the chemical composition is similar to plasma but does not contain coagulation protein. We performed detection of thrombin in 10-fold-diluted serum samples under the optimal conditions. The average recovery test was made by using the standard addition method. All data were collected from three independent measurements. From Table 1, it can be seen that the recoveries based on our method in the real samples were between 103 and 105 %. The relative standard deviations (RSD) were not higher than 3.2 %, indicating that the accuracy and precision of the method were satisfactory.

Conclusion

In summary, we have developed a simple NIR fluorescence assay using thrombin binding aptamer and Zn(II)-activated $CuInS_2$ Q-dots for the highly selective and sensitive detection of thrombin. The method is simple and fast, and exhibits excellent selectivity for thrombin in the presence of other proteins. We successfully detected thrombin in human serum samples with satisfactory results. Under the optimum conditions, a linear range for thrombin detection is found in the concentration of 0.034–102 nmol L^{-1} with a detection limit of 0.012 nmol L^{-1}. The ability of this method to detect thrombin at picomolar levels holds great potential in the diagnosis of diseases associated with coagulation abnormalities and cancers.

Acknowledgments This work was financially supported by the National Natural Science Foundation of China (No. 21075050, No. 21275063) and the science and technology development project of Jilin province, China (No. 20110334).

References

1. Shuman MA (1986) Thrombin-cellular interactions. Ann NY Acad Sci 485:228–239
2. Xue YH, Zhang XF, Dong QZ, Sun JA, Dai C, Zhou HJ, Ren N, Jia HL, Ye QH, Qin LX (2010) Thrombin is a therapeutic target for metastatic osteopontin-positive hepatocellular carcinoma. Hepatology 52:2012–2022
3. Oroval M, Climent E, Coll C, Eritja R, Avino A, Marcos MD, Sancenon F, Martinez-Manez R, Amoros P (2013) An aptamer-gated silica mesoporous material for thrombin detection. Chem Commun 49:5480–5482
4. Ebert MPA, Lamer S, Meuer J, Malfertheiner P, Reymond M, Buschmann T, Rocken C, Seibert V (2005) Identification of the thrombin light chain A as the single best mass for differentiation of gastric cancer patients from individuals with dyspepsia by proteome analysis. J Proteome Res 4:586–590
5. Xu H, Mao X, Zeng QX, Wang SF, Kawde AN, Liu GD (2009) Aptamer-functionalized gold nanoparticles as probes in a dry-reagent strip biosensor for protein analysis. Anal Chem 81:669–675
6. Li LD, Zhao HT, Chen ZB, Mu XJ, Guo L (2010) Aptamer-based electrochemical approach to the detection of thrombin by modification of gold nanoparticles. Anal Bioanal Chem 398:563–570
7. Hu J, Zheng PC, Jiang JH, Shen GL, Yu RQ, Liu GK (2009) Electrostatic interaction based approach to thrombin detection by surface-enhanced raman spectroscopy. Anal Chem 81:87–93
8. Bo FL, Gao BX, Duan WF, Li HX, Liu HM, Bai QQ (2013) Assembly-disassembly driven "off-on" fluorescent perylene bisimide probes for detecting and tracking of proteins in living cells. RSC Adv 3:17007–17010
9. Raichlin S, Sharon E, Freeman R, Tzfati Y, Willner I (2011) Electron-transfer quenching of nucleic acid-functionalized CdSe/ZnS quantum dots by doxorubicin: a versatile system for the optical detection of DNA, aptamer-substrate complexes and telomerase activity. Biosens Bioelectron 26:4681–4689
10. Liao DL, Chen J, Li WY, Zhang QF, Wang FY, Li YX, Yu C (2013) Fluorescence turn-on detection of a protein using cytochrome c as a quencher. Chem Commun 49:9458–9460
11. Zhang CL, Xu J, Zhang SM, Ji XH, He ZK (2012) One-pot synthesized DNA-CdTe quantum dots applied in a biosensor for the detection of sequence-specific oligonucleotides. Chem Eur J 18: 8296–8300
12. Iliuk AB, Hu LH, Tao WA (2011) Aptamer in bioanalytical applications. Anal Chem 83:4440–4452
13. Tang QJ, Su XD, Loh KP (2007) Surface plasmon resonance spectroscopy study of interfacial binding of thrombin to antithrombin DNA aptamers. J Colloid Interface Sci 315:99–106
14. Shan Y, Xu JJ, Chen HY (2011) Enhanced electrochemiluminescence quenching of CdS:Mn nanocrystals by CdTe QDs-doped silica nanoparticles for ultrasensitive detection of thrombin. Nanoscale 3:2916–2923
15. Bock LC, Griffin LC, Latham JA, Vermaas EH, Toole JJ (1992) Selection of single-stranded DNA molecules that bind and inhibit human thrombin. Nature 355:564–566

16. Smirnov I, Shafer RH (2000) Effect of loop sequence and size on DNA aptamer stability. Biochemistry 39:1462–1468
17. Zhang Y, Hong G, Zhang Y, Chen G, Li F, Dai H, Wang Q (2012) Ag2S quantum dot: a bright and biocompatible fluorescent nanoprobe in the second near-infrared window. ACS Nano 6: 3695–3702
18. Gao J, Chen K, Xie R, Xie J, Yan Y, Cheng Z, Peng X, Chen X (2010) In vivo tumor-targeted fluorescence imaging using near-infrared non-cadmium quantum dots. Bioconjug Chem 21:604–609
19. Park J, Dvoracek C, Lee KH, Galloway JF, Bhang HC, Pomper MG, Searson PC (2011) CuInSe/ZnS core/shell NIR quantum dots for biomedical imaging. Small 7:3148–3152
20. Au GHT, Shih WY, Tseng SJ, Shih WH (2012) Aqueous CdPbS quantum dots for near-infrared imaging. Nanotechnology 23: 275601–275609
21. Xie RG, Rutherford M, Peng XG (2009) Formation of high-quality I-III-VI semiconductor nanocrystals by tuning relative reactivity of cationic precursors. J Am Chem Soc 131:5691–5697
22. Liu SY, Li YY, Su XG (2012) Determination of copper(II) and cadmium(II) based on ternary $CuInS_2$ quantum dots. Anal Methods 4:1365–1370
23. Chen YF, Rosenzweig Z (2002) Luminescent CdS quantum dots as selective ion probes. Anal Chem 74:5132–5138
24. Niu SY, Qu LJ, Zhang Q, Lin JH (2012) Fluorescence detection of thrombin using autocatalytic strand displacement cycle reaction and a dual-aptamer DNA sandwich assay. Anal Biochem 421:362–367
25. Booth M, Brown AP, Evans SD, Critchley K (2012) Determining the concentration of CuInS2 quantum dots from the size-dependent molar extinction coefficient. Chem Mater 24:2064–2070
26. Yu WW, Qu LH, Guo WZ, Peng XG (2003) Experimental determination of the extinction coefficient of CdTe, CdSe, and CdS nanocrystals. Chem Mater 15:2854–2860
27. Xie R, Rutherford M, Peng X (2009) Formation of high-quality I− III− VI semiconductor nanocrystals by tuning relative reactivity of cationic precursors. J Am Chem Soc 131:5691–5697
28. Zhao Q, Lu X, Yuan C-G, Li X-F, Le XC (2009) Aptamer-linked assay for thrombin using gold nanoparticle amplification and inductively coupled plasma−mass spectrometry detection. Anal Chem 81:7484–7489
29. Chen Q, Tang W, Wang DZ, Wu XJ, Li N, Liu F (2010) Amplified QCM-D biosensor for protein based on aptamer-functionalized gold nanoparticles. Biosens Bioelectron 26:575–579
30. Li JWJ, Fang XH, Tan WH (2002) Molecular aptamer beacons for real-time protein recognition. Biochem Biophys Res Commun 292: 31–40
31. Zhang Y, Tian J, Zhai J, Luo Y, Wang L, Li H, Sun X (2011) Fluorescence-enhanced potassium ions detection based on inherent quenching ability of deoxyguanosines and K+−induced conformational transition of G-rich ssDNA from duplex to G-quadruplex structures. J Fluoresc 21:1841–1846
32. Uhrovcik J (2014) Strategy for determination of LOD and LOQ values—some basic aspects. Talanta 119:178–180